

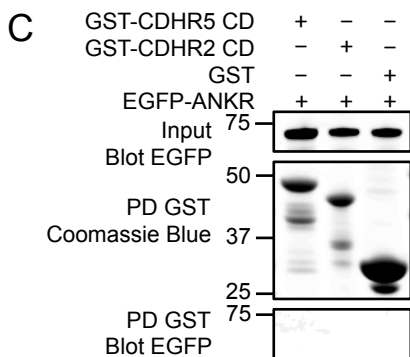
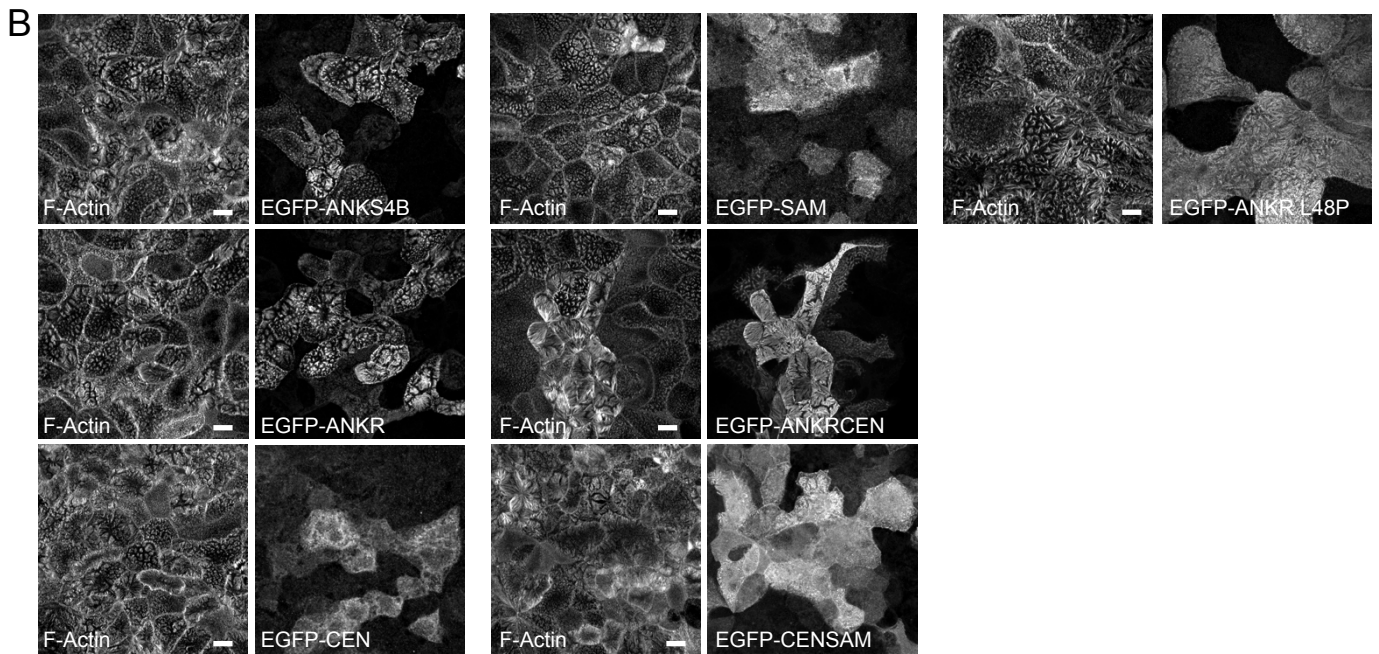
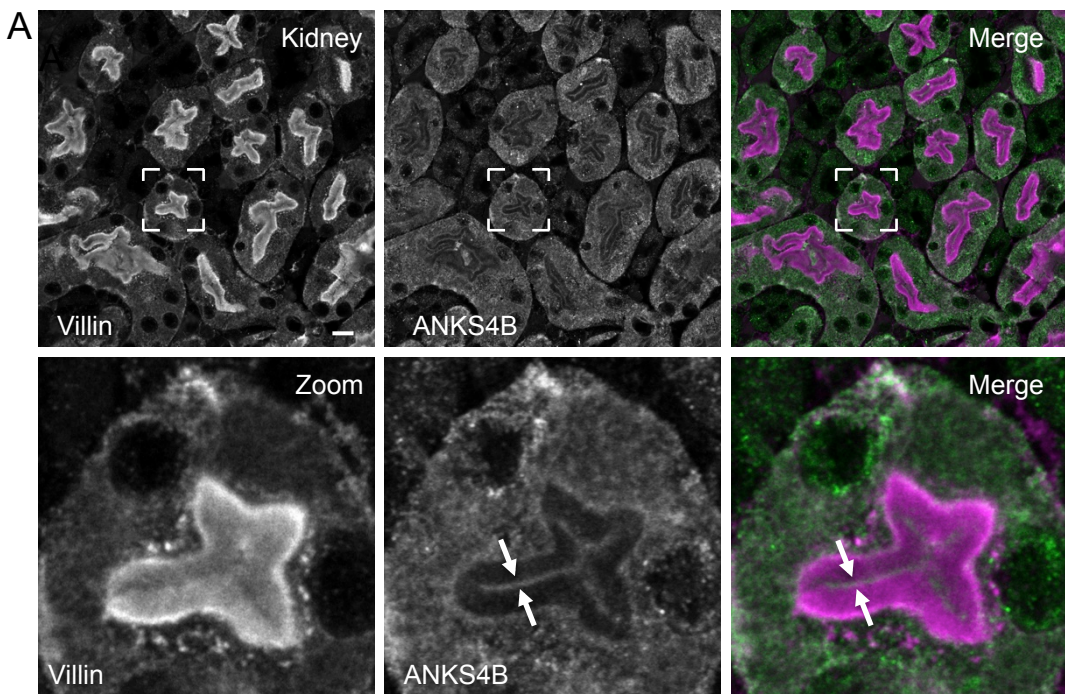
## SUPPLEMENTARY FIGURE LEGENDS

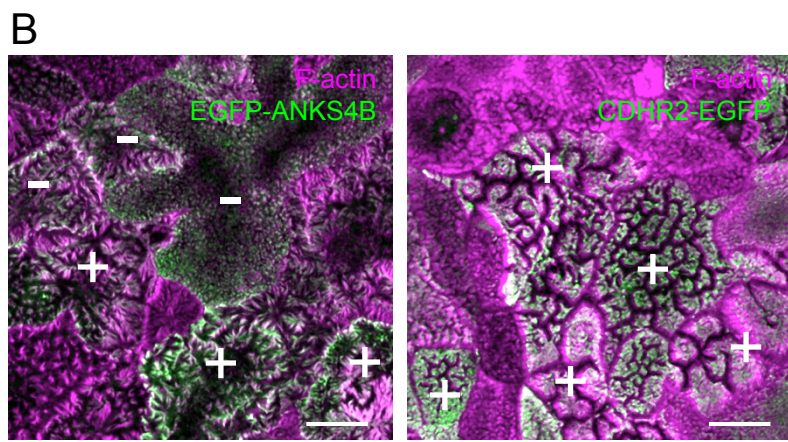
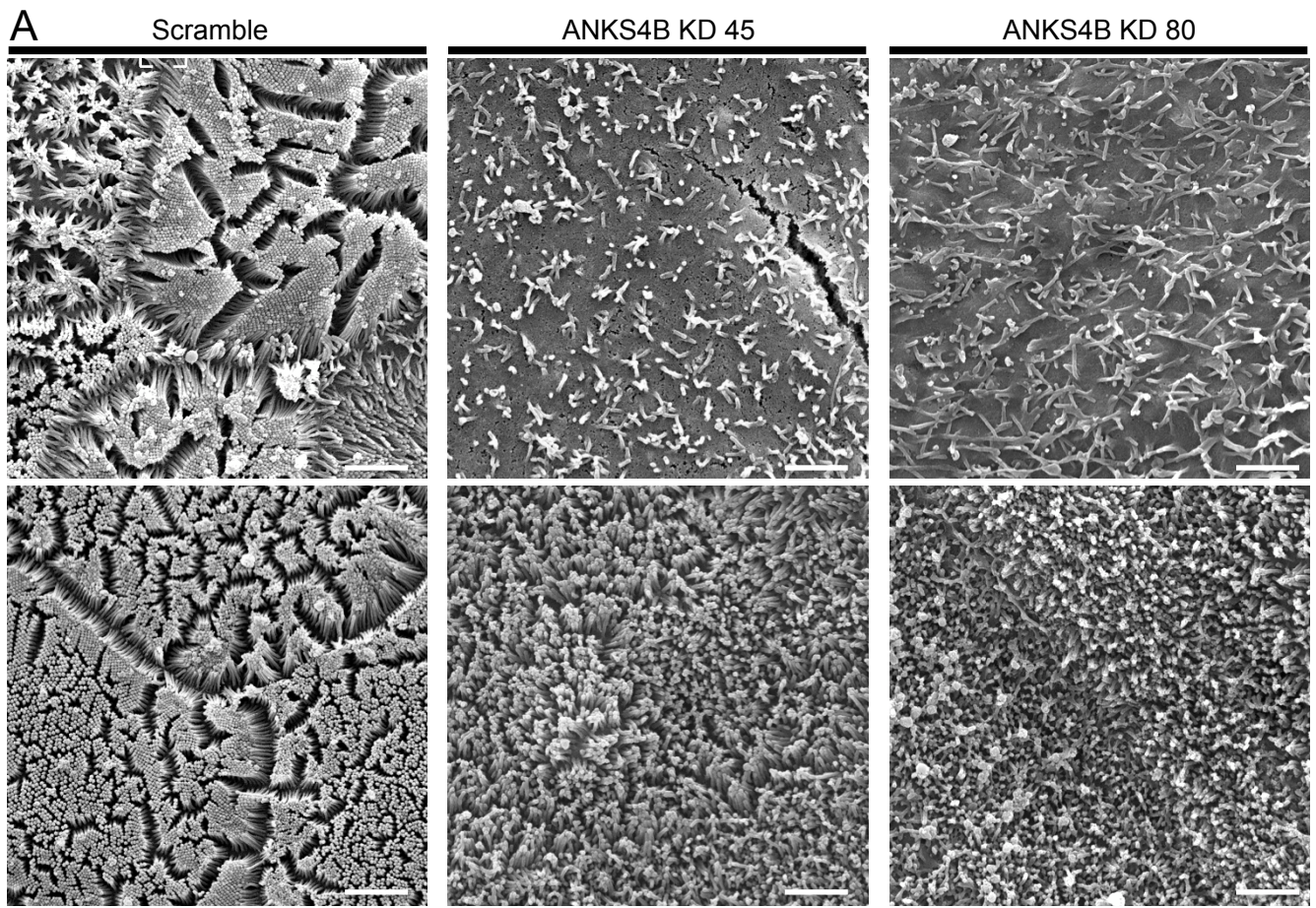
**Figure S1. Endogenous ANKS4B localization in mouse kidney tissue and domain construct expression in CACO-2<sub>BBE</sub> cells, related to Figure 1 and Figure 2.** (A) Confocal microscopy of mouse kidney tissue stained for ANKS4B (green) and villin (magenta). Boxed regions denote area in zoomed image panels. Arrows point to the distal tips of BB microvilli. Scale bar, 40  $\mu\text{m}$ . (B) Single channel versions of confocal images presented in Fig. 2B-H. Scale bars, 10  $\mu\text{m}$ . (C) Pull-downs of CDs of CDHR2 and CDHR5 fused to GST with the EGFP-tagged ANKR domain of ANKS4B. GST alone was used a control.

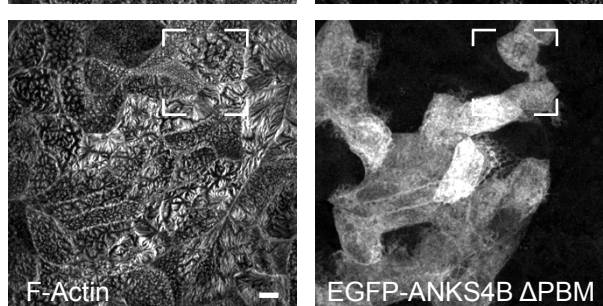
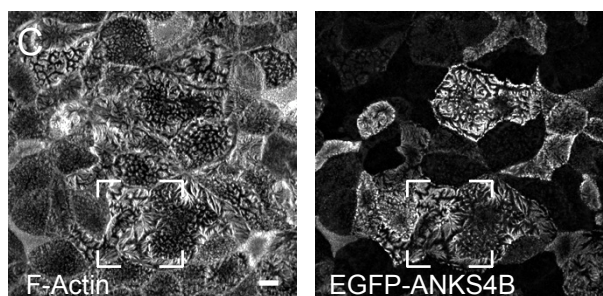
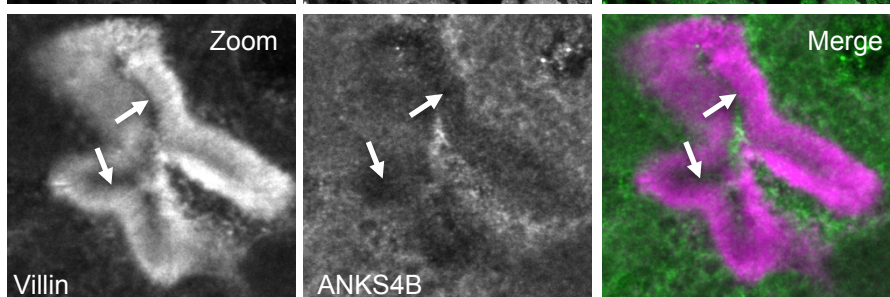
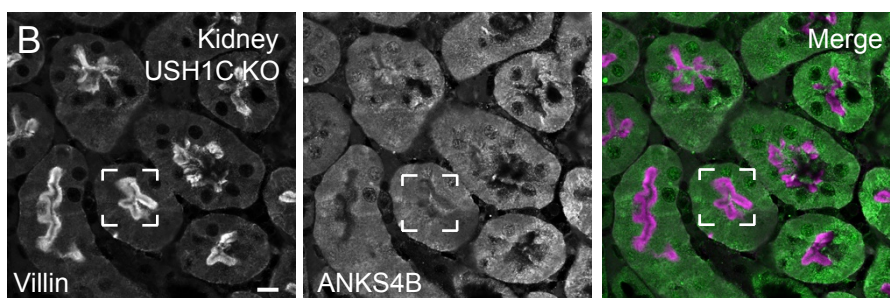
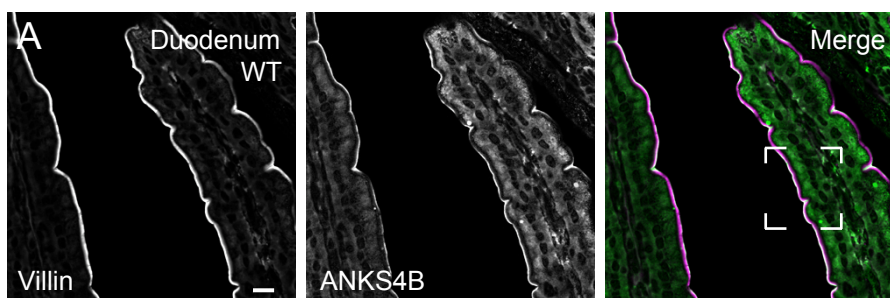
**Figure S2. Knockdown and overexpression of ANKS4B in CACO-2<sub>BBE</sub> cells, related to Figure 3.** (A) Additional SEM images of 20 DPC CACO-2<sub>BBE</sub> cells stably expressing either a scramble shRNA construct (*left*) or two independent shRNAs targeting ANKS4B (*middle* and *right*). Scale bars, 1  $\mu\text{m}$ . (B) Confocal images of 12 DPC CACO-2<sub>BBE</sub> monolayers stably expressing EGFP-ANKS4B (*left*) or CDHR2-EGFP (*right*). Plus signs highlight EGFP-tagged construct expressing cells with robust microvillar clustering; minus signs indicate cells that are over-expressing the EGFP-tagged construct, but do not exhibit strong microvilli clustering.

**Figure S3. Characterization of the functional interactions between ANKS4B and other IMAC components, related to Figure 4 and Figure 5.** (A) Single and merged channel, low magnification versions of confocal images presented in Fig. 4C. Tissue is stained for ANKS4B (green) and villin (magenta). Boxed regions denote zoomed areas presented in Fig 4C. Scale bars, 40  $\mu\text{m}$ . (B) Confocal microscopy of USH1C KO mouse kidney tissue stained for ANKS4B (green) and villin (magenta). Boxed regions denote area in zoomed image panels. Arrows point to the distal tips of BB microvilli. Scale bars, 40  $\mu\text{m}$ . (C) Single channel, low magnification versions of confocal images presented in Fig. 4F. Scale bars, 10  $\mu\text{m}$ . (D) Pull-down analysis of ANKS4B sub-domains with the MYO7B SH3MF2 tail fragment. FLAG-tagged MYO7B SH3MF2 tail served as bait where as EGFP-tagged fragments of ANKS4B served as prey. (E) Pull-down analysis of MYO7B tail domain constructs with USH1C. FLAG-tagged MYO7B tail fragments served as bait where as myc-tagged USH1C served as prey. (F) Pull-down analysis of ANKS4B sub-domains with the full-length tail of MYO7B. FLAG-tagged MYO7B full-length tail served as bait where as EGFP-tagged fragments of ANKS4B served as prey.

**Figure S4. ANKS4B is required for proper localization of other IMAC components in CACO-2<sub>BBE</sub> cells, related to Figure 6.** (A) Single channel versions of confocal images presented in Fig. 6A. Scale bars, 10  $\mu\text{m}$ .

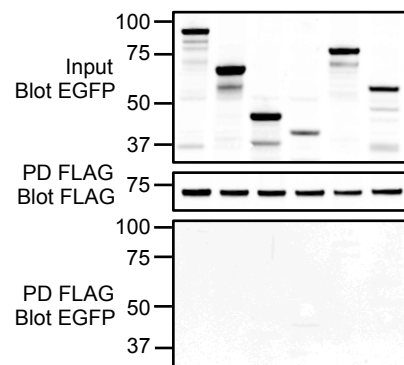






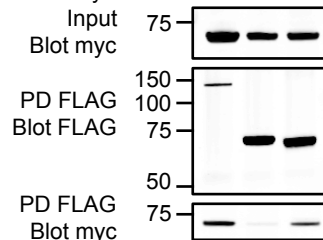
**D**

FLAG-MYO7B-SH3MF2	+	+	+	+	+	+
EGFP-ANKS4B	+	-	-	-	-	-
EGFP-ANKR	-	+	-	-	-	-
EGFP-CEN	-	-	+	-	-	-
EGFP-SAM	-	-	-	+	-	-
EGFP-ANKRCEN	-	-	-	-	+	-
EGFP-CENSAM	-	-	-	-	-	+



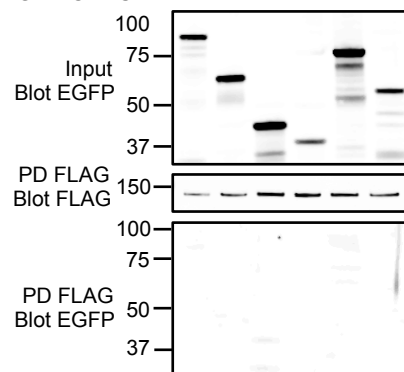
**E**

FLAG-MYO7B-full tail	+	-	-
FLAG-MYO7B-MF1SH3	-	+	-
FLAG-MYO7B-SH3MF2	-	-	+
myc-USH1C	+	+	+

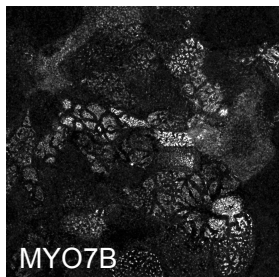
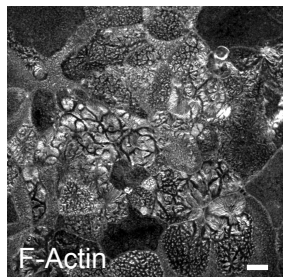
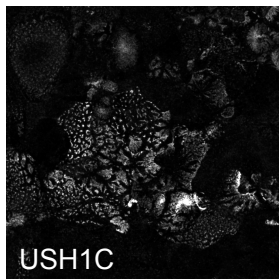
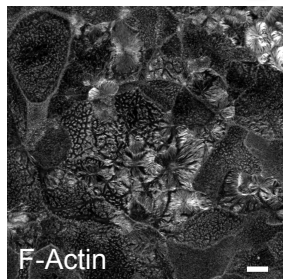
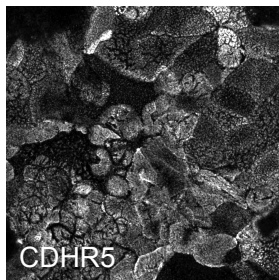
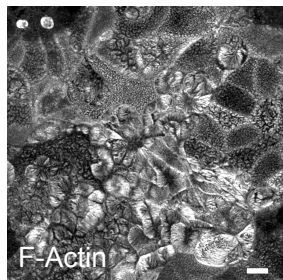
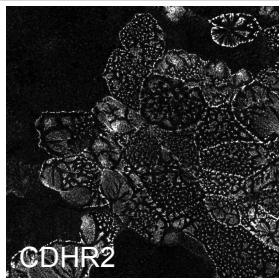
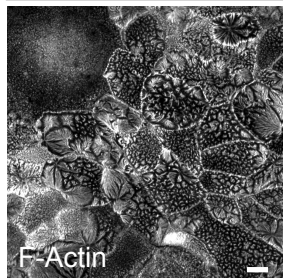


**F**

FLAG-MYO7B-full tail	+	+	+	+	+	+
EGFP-ANKS4B	+	-	-	-	-	-
EGFP-ANKR	-	+	-	-	-	-
EGFP-CEN	-	-	+	-	-	-
EGFP-SAM	-	-	-	+	-	-
EGFP-ANKRCEN	-	-	-	-	+	-
EGFP-CENSAM	-	-	-	-	-	+



## Scramble



## ANKS4B KD

